

Investigation of the high Curie temperature in $\text{Sr}_2\text{CrReO}_6$ J. M. De Teresa,^{1,*} D. Serrate,¹ C. Ritter,² J. Blasco,¹ M. R. Ibarra,¹ L. Morellon,¹ and W. Tokarz¹¹*Instituto de Ciencia de los Materiales de Aragón, Universidad de Zaragoza-CSIC, Facultad de Ciencias, Zaragoza, 50009, Spain*²*Institute Laue-Langevin, Grenoble Cedex, 38042, France*

(Received 23 November 2004; published 30 March 2005)

A detailed neutron diffraction study of $\text{Sr}_2\text{Fe}_{1-x}\text{Cr}_x\text{ReO}_6$ half-metallic double perovskites has been carried out. With increasing Cr content, the temperature for the cubic-tetragonal transition decreases ($T_t \approx 490$ K for $x=0$ and ≈ 260 K for $x=1$) and the cell volume shrinks more than 2% while the Curie temperature increases substantially ($T_C \approx 420$ K for $x=0$ and ≈ 620 K for $x=1$). We discuss the origin of the anomalously high T_C of $\text{Sr}_2\text{CrReO}_6$ in terms of structural and band hybridization effects.

DOI: 10.1103/PhysRevB.71.092408

PACS number(s): 75.47.-m, 61.12.Ld, 75.30.Kz, 72.25.-b

The search for half-metallic compounds having a high Curie temperature (T_C) for applications in spintronics has been intense in recent years. Half-metallic compounds provide conduction electrons with only one spin direction at the Fermi level, which normally optimizes the output of spintronic devices. In order to build devices operational at room temperature, materials with high T_C are required. Only a few oxides, semiconductors, and metallic alloys are candidates to show half-metallicity.¹ This is the reason why the finding of new half-metallic materials with high T_C is very important. Promising compounds are found in the family of the so-called “double-perovskite” oxides. These compounds have the general formula $\text{ABB}'\text{O}_6$ with ordering of the B and B' cations and some of them are metallic as required for magnetoelectronic applications. Amongst the metallic compounds, $\text{Sr}_2\text{FeMoO}_6$ was reported to show half-metallicity and a T_C of 420 K caused by an indirect ferromagnetic $\text{Fe}(t_{2g})\text{—O—Mo}(t_{2g})$ interaction.² Band calculations indicate that the t_{2g} spin-up subband is below the Fermi level and consists of five “localized” $3d$ electrons produced by Fe ($S=5/2$). The t_{2g} spin-down subband is located at the Fermi level (E_F) and contains one “delocalized” electron shared by Fe and Mo and mediating the indirect ferromagnetic interaction between the “localized” spins through the oxygen orbitals. Ideally, the conduction electrons should show complete negative spin polarization at the Fermi level resulting in the so-called half-metallicity. A similar T_C was reported for the $\text{Sr}_2\text{FeReO}_6$ compound, studied with neutrons by Auth *et al.*³ Philipp *et al.* reported a T_C of 458 K for Sr_2CrWO_6 .⁴ But the highest T_C for this type of compounds has been reported for $\text{Sr}_2\text{CrReO}_6$ ($T_C=620$ K).⁵ Interest in this compound has furthermore strongly increased as high-quality metallic thin films of $\text{Sr}_2\text{CrReO}_6$ can be grown by sputtering techniques,⁶ which opens exciting applications in spintronic devices based on this compound. In order to investigate the structural and magnetic properties of $\text{Sr}_2\text{CrReO}_6$ and correlate them with the high T_C , we have carried out a thorough neutron diffraction study of the $\text{Sr}_2\text{Fe}_{1-x}\text{Cr}_x\text{ReO}_6$ series in the temperature range 5–700 K. In a recent report Kato *et al.* have studied with neutron diffraction the structural properties at room temperature of the $\text{Sr}_2\text{FeReO}_6$ and $\text{Sr}_2\text{CrReO}_6$ compounds.⁷ Within the error bars of the experiments, our results at room temperature in both compounds coincide with those of Ref. 7.

The polycrystalline samples with nominal Cr concentration $x(\text{Cr})=0, 0.25, 0.5, 0.75, 0.9,$ and 1 have been synthesized with the solid-state technique. Stoichiometric amounts of $\text{Sr}_2\text{CO}_3, \text{Fe}_2\text{O}_3, \text{ReO}_3$ and Re (ReO_3/Re ratio is $5/1$), and Cr_2O_3 were mixed and pressed into pellets. The pellets were heated at 1000°C for 3 h in an atmosphere of Ar with heating and cooling rates of $7^\circ\text{C}/\text{min}$. X-ray diffraction was performed with a D-Max Rigaku system with rotating anode. Magnetization measurements were performed by using a superconducting quantum interference device magnetometer. Neutron diffraction experiments were performed on two different instruments at the high flux reactor in the Institute Laue-Langevin (Grenoble, France): D1B ($\lambda=2.52$ Å) and the high resolution D2B ($\lambda=1.594$ Å).

X-ray diffraction at room temperature and neutron diffraction on D2B in the paramagnetic phase at $T=650\text{--}700$ K have been used to refine the sample stoichiometry and the amount of BB' antisite defects. This is important in order to correctly interpret as well the low temperature data where the compounds become tetragonal and magnetic. We have found that the compounds with $x=0$ and 1 are stoichiometric except for tiny impurities below 1%. In the case of $x=0$ no antisite defects exist whereas for $x=1$ an amount of $\approx 10\%$ of antisites was found in neutron measurements and $\approx 12\%$ of antisites in x-ray measurements. For the intermediate Cr concentrations, secondary phases of the same structural type exist. For $x=0.5$, the main phase (80%) is close to the expected one [$\text{Sr}_2\text{Fe}_{0.43(2)}\text{Cr}_{0.57(2)}\text{ReO}_6$] and antisites are not detectable. The second phase (20%) is an Fe-rich one [$\text{Sr}_2\text{FeReO}_6$]. For $x=0.75$, the main phase (70%) is close to the expected one [$\text{Sr}_2(\text{Fe}_{0.14}\text{Cr}_{0.81(2)}\text{Re}_{0.05(1)})(\text{Re}_{0.95(2)}\text{Cr}_{0.05})\text{O}_6$] with $\approx 5\%$ antisites. The second phase (30%) is also an Fe-rich one [$\text{Sr}_2\text{Fe}_{0.85(3)}\text{Cr}_{0.15(3)}\text{ReO}_6$]. Finally, for $x=0.9$ the main phase (90%) is close to the expected one [$\text{Sr}_2(\text{Fe}_{0.1}\text{Cr}_{0.83(2)}\text{Re}_{0.07(2)})(\text{Re}_{0.90(2)}\text{Cr}_{0.10(2)})\text{O}_6$] with $\approx 10\%$ antisites. The second phase (10%) is again an Fe-rich one [$\text{Sr}_2\text{Fe}_{0.85}\text{Cr}_{0.15}\text{ReO}_6$]. We note that in order to get the final stoichiometries of the main phase in the intermediate Cr content compounds, we have assumed that only the Cr ions (with ionic radius closer to Re) and not the Fe ions (with larger ionic radius than Re) can be misplaced on the Re sites (as Fe and Re have similar scattering lengths, they can be hardly distinguished with neutrons). From the neutron Ri-

TABLE I. Selected data of the main phase of the $\text{Sr}_2\text{Fe}_{1-x}\text{Cr}_x\text{ReO}_6$ compounds obtained from the Rietveld refinement of the neutron diffraction measurements. For all the compounds, the space group at 650 K is cubic $Fm\bar{3}m$ and at 5 K is tetragonal $I4/m$.

	T (K)	$x=0$	$x=0.5$	$x=0.75$	$x=0.9$	$x=1$
a (Å)	650	5.5932(5)	5.5754(1) ^a	5.5585(1) ^a	5.5550(1)	5.54950(7)
a (Å)	5	5.5408(1)	5.5315(2)	5.5231(17)	5.5243(5)	5.5206(4)
c (Å)	5	7.9156(2)	7.87693(2)	7.8231(1)	7.8125(12)	7.8023(1)
Fe(Cr)—O (Å)	650	2.009(3)	1.989(3) ^a	1.9778(50) ^a	1.981(2)	1.965(3)
Fe(Cr)—O ₁ (Å)	5	1.959(7)	1.968(5)	1.975(8)	1.978(13)	1.961(3)
Fe(Cr)—O ₂ (Å)	5	2.049(5)	2.049(7)	1.994(18)	1.958(38)	1.951(0)
Re—O (Å)	650	1.946(3)	1.954(3) ^a	1.9526(50) ^a	1.947(2)	1.959(3)
Re—O ₁ (Å)	5	1.986(7)	1.955(5)	1.939(8)	1.938(14)	1.952(3)
Re—O ₂ (Å)	5	1.909(5)	1.881(7)	1.918(18)	1.948(38)	1.951(0)
Fe(Cr)—O ₁ —Re (deg.)	5	166.6(3)	171.1(2)	172.1(3)	172.0(5)	171.9(1)
Fe(Cr) moment (μ_B)	5	4.35(6)	3.44(7)	2.87(8)	2.67(8)	2.52(1)
Re moment (μ_B)	5	-0.16(7)	-0.37(9)	-0.47(9)	-0.58(9)	-0.21(11)

^aData taken at 700 K.

etveld refinement of the patterns obtained on D1B and the high-resolution D2B at selected temperatures, the space group, lattice parameters, bond angles, atom distances, and magnetic moments have been determined (see some selected data in Table I). For the intermediate Cr content compounds, only the results for the main phase will be discussed. As an example, we show in Fig. 1 the measurement on D2B and the corresponding refinement at 5 K of the $\text{Sr}_2\text{CrReO}_6$ compound. At 650 K all the compounds are cubic ($Fm\bar{3}m$) and paramagnetic. When decreasing the temperature, two types of transitions are detected: the paramagnetic-ferromagnetic transition at T_C and the cubic-tetragonal ($I4/m$) transition at T_t . Both transitions are clearly decoupled as in doped $\text{Sr}_2\text{FeMoO}_6$ (Ref. 8) and in contrast to the behavior in pure $\text{Sr}_2\text{FeMoO}_6$.⁹ Figure 2 shows the dependence of T_C and T_t on the Cr content: whereas T_t decreases from ≈ 490 K for $x=0$ down to ≈ 260 K for $x=1$, T_C increases from ≈ 420 K for

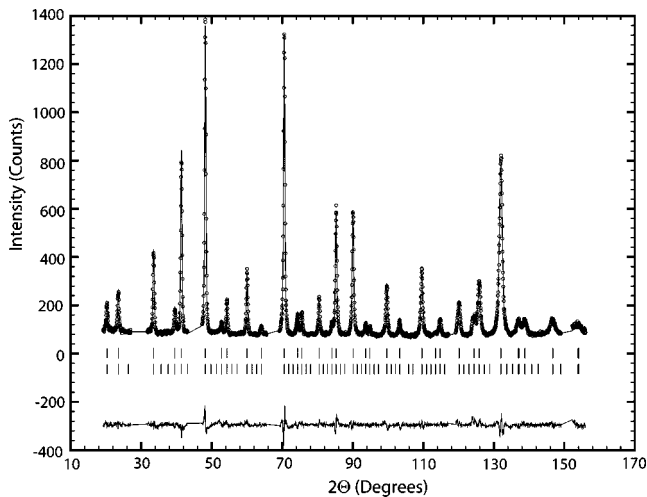


FIG. 1. Experimental data and Rietveld refinement of the neutron diffraction pattern of $\text{Sr}_2\text{CrReO}_6$ at 5 K taken in D2B. Some regions of the pattern have been excluded which included a peak from the cryostat and very small impurity peaks from an unknown volatile contaminant.

$x=0$ up to ≈ 620 K for $x=1$. Figure 2 also shows the temperature evolution of the Fe(Cr)—O₁—Re angle for $\text{Sr}_2\text{FeReO}_6$ and $\text{Sr}_2\text{CrReO}_6$, which deviates from 180° below T_t . This angle is at the lowest temperature (5 K) equal to 166.5° for $x=0$ and 172° for $x=1$, which indicates that Cr doping distorts the structure less from cubic. The tolerance factor, $f=d(\text{Sr—O})/d(\text{Fe/Cr/Re—O})/\sqrt{2}$, which reflects the overall size mismatch of the cations and can give rise to changes of the space group if different from $f=1$, is approximately identical ($f \approx 1$) for $\text{Sr}_2\text{FeReO}_6$ and $\text{Sr}_2\text{CrReO}_6$ according to our neutron data at 650 K. However, a better cation size matching in $\text{Sr}_2\text{CrReO}_6$ is clear from the cation-oxygen distances. At 650 K, the Rietveld refinement gives for $\text{Sr}_2\text{FeReO}_6$ $d(\text{Fe—O})=2.009$ Å and $d(\text{Re—O})$

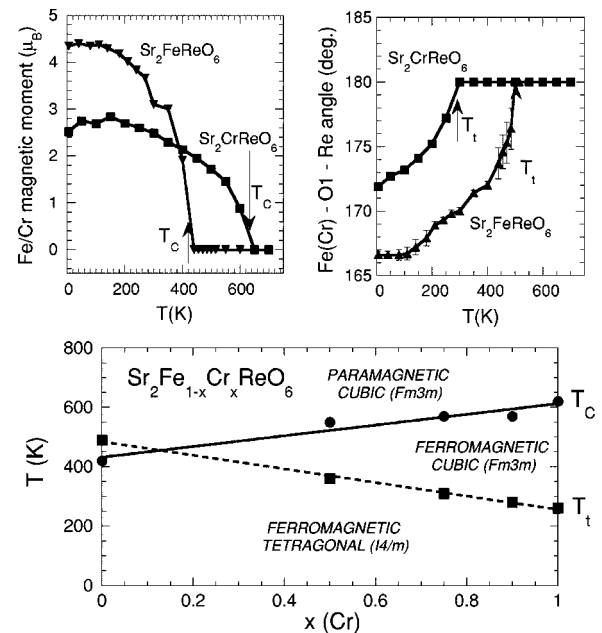


FIG. 2. Bottom panel: structural and magnetic phase diagram of $\text{Sr}_2\text{Fe}_{1-x}\text{Cr}_x\text{ReO}_6$. Top panels: Fe/Cr magnetic moment and Fe(Cr)—O₁—Re angle as a function of temperature for $x=0$ and 1.

$=1.946 \text{ \AA}$ whereas for $\text{Sr}_2\text{CrReO}_6$ it gives $d(\text{Cr—O}) = 1.965 \text{ \AA}$ and $d(\text{Re—O}) = 1.959 \text{ \AA}$. This reflects the more similar value of the ionic radius of the Cr ions than the Fe ions to the Re ions: in coordination VI, $r(\text{Fe}^{+3}) = 0.645 \text{ \AA}$, $r(\text{Cr}^{+3}) = 0.615 \text{ \AA}$, and $r(\text{Re}^{+5}) = 0.58 \text{ \AA}$.¹⁰ As a consequence, it is reasonable to find a less distorted structure with Cr doping (evidence for the importance of the BB' size matching for the stability of the cubic structure at fixed A -cation composition has been given in Ref. 8).

The spontaneous magnetic moment at the Fe(Cr) site as a function of temperature is also shown in Fig. 2 for $x=0$ and 1. In the case of $\text{Sr}_2\text{FeReO}_6$, the Fe magnetic moment at low temperature is $\approx 4.5 \mu_B$, which is an expected value for $\text{Fe}^{+2}/\text{Fe}^{+3}$ mixed valence in the high spin state ($4 \mu_B$ for Fe^{+2} and $5 \mu_B$ for Fe^{+3}). In $\text{Sr}_2\text{CrReO}_6$ the Cr magnetic moment at low temperature amounts to $\approx 2.5\text{--}3 \mu_B$, which is also an expected value for $\text{Cr}^{+2}/\text{Cr}^{+3}$ mixed valence ($2 \mu_B$ for low-spin Cr^{+2} and $3 \mu_B$ for high-spin Cr^{+3}). While in the case of Cr^{+3} , we expect to have three localized electrons in the spin-up t_{2g} orbitals, the fourth electron present in Cr^{+2} will plausibly go to the spin-down t_{2g} band [producing $\mu(\text{Cr}^{+2}) = 2 \mu_B$] as band calculations in the related compound Sr_2CrWO_6 indicate that the Cr spin-down t_{2g} band is at the Fermi level whereas the e_g level is 0.5 eV above E_F .⁴

The determination of the magnetic moment at the Re site is more difficult to obtain due to the uncertainties in the value of the magnetic form factor of Re and the substantial orbital moment of Re in Re-based double perovskites.¹¹ Similar results (within the error bars of the refinements) for the Re magnetic moment are obtained by using the magnetic form factor of Mo^{+3} (as done by Auth *et al.*³) or the magnetic form factors published by Oikawa *et al.*¹² and Popov *et al.*¹³ As a consequence, in the following we will report the values obtained by using the magnetic form factor of Mo^{+3} . A general trend is that we obtain magnetic moment values for Re much lower than expected. For example, for $\text{Sr}_2\text{FeReO}_6$ we obtain at $T=5 \text{ K}$ $\mu(\text{Re}) = -0.16(7) \mu_B$ (antiparallel to the Fe magnetic moment) whereas NMR measurements on the same compound indicates $\mu(\text{Re}) = -0.94 \mu_B$ (also antiparallel to the Fe magnetic moment).¹⁴ For $\text{Sr}_2\text{CrReO}_6$ we obtain at $T=100 \text{ K}$ $\mu(\text{Re}) = -0.32(10) \mu_B$ (antiparallel to the Fe magnetic moment) but specific studies with more appropriate tools (*x*-ray magnetic circular dichroism for example) should be carried out before concluding safely about the spin and orbital magnetic moment of Re in this series.

The obtained magnetic moment values at the Fe(Cr) site and the antiparallel alignment with the magnetic moment of Re are consistent with the ionic picture proposed for these compounds. Within this picture, as the Cr content is increased, the Fe(Cr) $3d$ spin-up subband below the Fermi level becomes depopulated from five electrons for $x=0$ down to three electrons for $x=1$. The two electrons provided by Re ions would go to the t_{2g} spin-down subband formed by hybridization of the Fe(Cr)- $3d$ - t_{2g} , O- $2p$, and Re- $5d$ - t_{2g} bands. These t_{2g} spin-down electrons would mediate the indirect ferromagnetic mechanism between Fe(Cr) and Re through oxygen ions and would be responsible for the metallic behavior measured in bulk and thin films of $\text{Sr}_2\text{CrReO}_6$.^{5,6} Magnetization measurements are also consistent with this

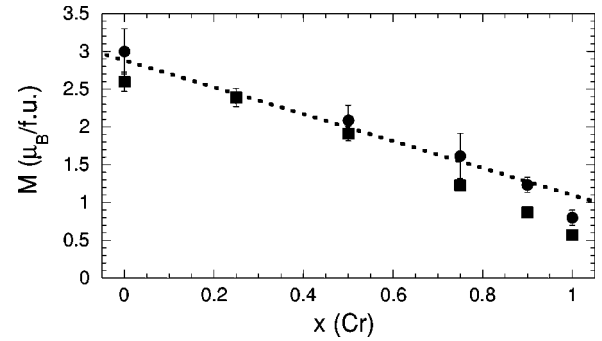


FIG. 3. Magnetization at 5 K under 5 T as a function of Cr content. Squares stand for the experimental data. Circles stand for the calculated magnetization according to the actual stoichiometry and antisites. The dashed line is the theoretical behavior.

picture. Within the ionic picture, the saturation magnetization should linearly decrease with the Cr doping from $3 \mu_B$ for $x=0$ down to $1 \mu_B$ for $x=1$. In Fig. 3, the experimental magnetization data at 5 K is shown as a function of the Cr content and compared to the calculated expected magnetization taking into account the actual sample stoichiometry and the level of antisites. We have used the following formula for the calculated magnetization: $m_{\text{cal}} = z_1(3-2x_1)(1-y_1) + z_2(3-2x_2)(1-y_2)$, where $z_{1(2)}$ is the percentage of the first (second) phase, $x_{1(2)}$ is the Cr content of the first (second) phase, and $y_{1(2)}$ is the antisite content of the first (second) phase. In general, the agreement between the experimental and calculated magnetization is reasonably good taking into account the error bars of the refined stoichiometries and level of antisites and the error bars of the magnetization measurements. The agreement is only moderate for the rich Cr samples. This could be linked to a smooth magnetic transition taking place below 200 K in the Cr-rich compounds detected with magnetization measurements. The performed neutron diffraction refinements also indicate a slight decrease in the value of the magnetic moment at the Fe(Cr) and Re sites below 200 K in the Cr-rich compounds (see Fig. 2 for $x=1$). However, due to the metrically cubic structure, it has not been possible to obtain precise information on the magnetic structure. Our magnetization measurements indicate that the coercivity and the saturation field increase considerably at this temperature and that a magnetic field of 5 T is not long enough to achieve saturation at 5 K for the Cr-rich compounds. This low-temperature magnetic transition and its impact on the transport properties will be addressed in detail in a future paper.

In Fig. 4 the cell volume is shown as a function of temperature along the whole series. A striking feature is the remarkable cell volume shrinkage that occurs with Cr doping. For $\text{Sr}_2\text{CrReO}_6$ the cell volume has decreased more than 2% when compared to $\text{Sr}_2\text{FeReO}_6$. This is a large value in terms of lattice effects. The reason for the lattice contraction can be found in the difference of the ionic radii of Fe and Cr ions. The ionic radii data of Ref. 10 in coordination VI for Cr and Fe indicate substantial differences in their respective values: low-spin- Cr^{+2} /high-spin- Cr^{+3} ($0.73 \text{ \AA}/0.615 \text{ \AA}$) and high-spin- Fe^{+2} /high-spin- Fe^{+3} ($0.78 \text{ \AA}/0.645 \text{ \AA}$). For example, in

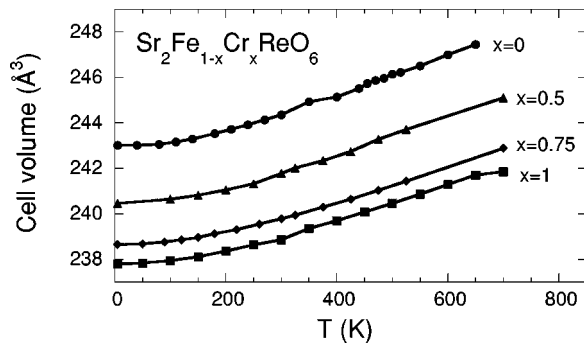


FIG. 4. Cell volume as a function of temperature in $\text{Sr}_2\text{Fe}_{1-x}\text{Cr}_x\text{ReO}_6$.

an electronic configuration close to the valence +3 state, the difference in the ionic radius between Cr^{+3} and Fe^{+3} can be around 5%. An additional effect due to changes in the valence state could be also contributing to the lattice contraction. In this sense, in Cr-doped $\text{Sr}_2\text{FeMoO}_6$, Cr replaces Fe as well mostly as Cr^{+3} .⁸

The anomalously large increase of T_C in the $\text{Sr}_2\text{Fe}_{1-x}\text{Cr}_x\text{ReO}_6$ series can be qualitatively explained by structural and band hybridization effects as discussed hereafter. In magnetic oxides with perovskite structure, T_C has been claimed to be controlled by the electronic bandwidth.^{15,9} The electronic bandwidth will plausibly depend on band hybridization terms, which will be also influenced by the structural parameters. In the case of e_g -active oxides (nickelates¹⁶ and manganites¹⁵) and t_{2g} -active oxides (titanates¹⁷), evidence for the influence of the structural parameters on the electronic bandwidth has been given. One useful way to estimate the electronic bandwidth is through a tight-binding model, which is straightforwardly applicable to transition-metal oxides with cubic perovskite structure.¹⁸ In the formalism developed by Harrison (and co-workers),¹⁸ there is a broadening of the O-2p and the transition-metal-3d levels due to the pd coupling which can be expressed through the band hybridization terms: $V_{pd\sigma} = -(3\sqrt{15}/2\pi)/(\hbar^2\sqrt{r_p r_d^3}/md^4)$ and $V_{pd\pi} = (3\sqrt{5}/2\pi)/(\hbar^2\sqrt{r_p r_d^3}/md^4)$, where r_d (d -state radius) and r_p

(p -state radius) are tabulated, respectively, for the transition metals and oxygen and d is the transition metal-oxygen distance. In the $\text{Sr}_2\text{Fe}_{1-x}\text{Cr}_x\text{ReO}_6$ series we can estimate the pd hybridization terms for the Fe(Cr)—O and Re—O bonds by using the r_d and r_p tabulated values¹⁸ and our neutron diffraction data at 600 K for the transition metal-oxygen distances (all the compounds being cubic at that temperature). In the case of the $\text{Sr}_2\text{FeReO}_6$ compound, the $V_{pd\sigma}$ and $V_{pd\pi}$ terms associated to the Fe—O bond are, respectively, -0.67 and 0.39 eV. For the Re—O bond, it amounts, respectively, to -1.56 and 0.90 eV. With Cr doping a small decrease of the hybridization coupling is obtained associated to the Re—O bond whereas a substantial enhancement is obtained associated to the Cr—O bond. For the $\text{Sr}_2\text{CrReO}_6$ compound the $V_{pd\sigma}$ and $V_{pd\pi}$ terms associated to the Cr—O bond are, respectively, -1.04 and 0.60 eV. For the Re—O bond, it amounts, respectively, to -1.53 and 0.88 eV. Contributions to the hybridization enhancement come from the shorter Cr—O bond length compared to Fe—O and the larger value of the d -state radius (r_d) in Cr than in Fe. We propose that the enhanced pd coupling (in other words, the larger bandwidth) will allow larger B—O—B' electron hopping integrals and, consequently, will reinforce the indirect ferromagnetic interaction and T_C .

In summary, our neutron and the magnetization results are consistent with the simple ionic picture proposed for $\text{Sr}_2\text{Fe}_{1-x}\text{Cr}_x\text{ReO}_6$ with itinerant electrons in the conduction band mediating an indirect effective ferromagnetic interaction between Fe(Cr) and Re through oxygen ions. Our neutron diffraction measurements indicate that Cr doping brings about a substantial cell volume reduction and improves the cation size matching. Together with the optimized structure, Cr doping enhances the pd band hybridization, which also contributes to the large T_C . Future theoretical calculations and experiments addressing the high T_C in $\text{Sr}_2\text{CrReO}_6$ and related new high- T_C double-perovskite compounds should take these findings into account.

Financial support by the European Project SCOOTMO and by the Spanish CICYT (MAT2002-04657 and MAT2002-01221, including FEDER funding) is acknowledged.

*Electronic address: deteresa@unizar.es

- ¹J. M. D. Coey and S. Sanvito, *J. Phys. D* **37**, 988 (2004).
- ²K.-I. Kobayashi, T. Kimura, H. Sawada, K. Terakura, and Y. Tokura, *Nature (London)* **395**, 677 (1998).
- ³K.-I. Kobayashi *et al.*, *Phys. Rev. B* **59**, 11 159 (1999); N. Auth *et al.*, *J. Magn. Magn. Mater.* **272–276**, 607(E) (2004).
- ⁴J. B. Philipp *et al.*, *Phys. Rev. B* **68**, 144431 (2003).
- ⁵H. Kato *et al.*, *Appl. Phys. Lett.* **81**, 328 (2002).
- ⁶H. Asano, N. Kozuka, A. Tsuzuki, and M. Matsui, *Appl. Phys. Lett.* **85**, 263 (2004).
- ⁷H. Kato *et al.*, *Phys. Rev. B* **69**, 184412 (2004).
- ⁸C. Ritter *et al.*, *Solid State Sci.* **6**, 419 (2004).
- ⁹C. Ritter, *et al.*, *J. Phys.: Condens. Matter* **12**, 8295 (2000).
- ¹⁰R. D. Shannon, *Acta Crystallogr., Sect. A: Cryst. Phys., Diffr., Theor. Gen. Crystallogr.* **A32**, 751 (1976).
- ¹¹J. M. De Teresa, D. Serrate, J. Blasco, M. R. Ibarra, and L. Mollon, *Phys. Rev. B* **69**, 144401 (2004).

- ¹²K. Oikawa, T. Kamiyama, H. Kato, and Y. Tokura, *J. Phys. Soc. Jpn.* **72**, 1411 (2003).
- ¹³G. Popov *et al.*, *J. Phys.: Condens. Matter* **16**, 135 (2004).
- ¹⁴Cz. Kapusta *et al.*, *J. Magn. Magn. Mater.* **272–276**, 1619(E) (2004).
- ¹⁵P. G. Radaelli *et al.*, *Phys. Rev. B* **56**, 8265 (1997); G. M. Zhao, K. Conder, H. Keller, and K. A. Müller, *Nature (London)* **381**, 676 (1996).
- ¹⁶J. B. Torrance, P. Lacorre, A. I. Nazzari, E. J. Ansaldo, and Ch. Niedermayer, *Phys. Rev. B* **45**, R8209 (1992); M. Medarde *et al.*, *ibid.* **52**, 9248 (1995).
- ¹⁷Y. Okimoto, T. Katsufuji, Y. Okada, T. Arima, and Y. Tokura, *Phys. Rev. B* **51**, 9581 (1995); M. Imada, A. Fujimori, and Y. Yokura, *Rev. Mod. Phys.* **70**, 1039 (1998).
- ¹⁸W. A. Harrison, *Elementary Electronic Structure* (World Scientific, Singapore, 1999).